Rhodium(III) Complexes with Acyclic Tetrathioether Ligands. Effects of Backbone Chain Length on the Conformation of the Rh(III) Complex

Niranjan Goswami,[†] Roger Alberto,[‡] Charles L. Barnes,[†] and Silvia Jurisson*[,†]

Department of Chemistry, University of Missouri, Columbia, Missouri 65211, and Division of Radiopharmacy, Paul Scherrer Institut, Wurenlingen and Villigen, CH-5232 Villigen PSI, Switzerland

Received August 8, 1996[⊗]

Several Rh(III) complexes containing tetradentate thioether ligands of the general form $[RhCl_2(RCH_2S(CH_2)_nS(CH_2)_mS(CH_2)_nSCH_2R)]X$ (n, $m = 2$ or 3; R = COOH, C_6H_5; X = Cl^-, PF_6^-, BPh_4^-) have been synthesized and fully characterized. The effect of the ligand backbone size on the configuration (*cis* or *trans*) has been investigated. The smaller backbone chain length favored the *cis* isomer (n, $m = 2$, *cis*; $n = 3$, $m = 2$ or n, $m = 3$, *trans*). However, both *cis* and *trans* isomers were observed in the case where $n = 2$ and $m = 3$. Spectroscopic methods (UV−visible and NMR) were used to characterize the solution conformations of these complexes, and single-crystal X-ray diffraction analyses determined the solid state structures of the benzyl derivatives. *cis*-$[RhCl_2(PhCH_2S(CH_2)_2S(CH_2)_2S(CH_2)_2SCH_2Ph]PF_6$ crystallized in the monoclinic space group $P2_1/c$ with $a = 14.365(2)$ Å, $b = 13.200(3)$ Å, $c = 15.736(2)$ Å, $\beta = 115.571(4)°$, $Z = 4$, $R = 0.048$ and $R_w = 0.057$. *trans*-$[RhCl_2(PhCH_2S(CH_2)_2S(CH_2)_3S(CH_2)_2SCH_2Ph]PF_6$ crystallized in the monoclinic space group $P2_1/c$ with $a = 10.937(3)$ Å, $b = 19.055(2)$ Å, $c = 13.734(4)$ Å, $\beta = 103.596(13)°$, $Z = 4$, $R = 0.037$ and $R_w = 0.046$. *trans*-$[RhCl_2(PhCH_2S(CH_2)_3S(CH_2)_2S(CH_2)_3SCH_2Ph]PF_6$ crystallized in the triclinic space group $P\bar{1}$ with $a = 7.732(2)$ Å, $b = 13.046(3)$ Å, $c = 15.720(2)$ Å, $\alpha = 67.62(2)°$, $\beta = 79.63(2)°$, $\gamma = 78.60(2)°$, $Z = 2$, $R = 0.049$ and $R_w = 0.061$. *trans*-$[RhCl_2(PhCH_2S(CH_2)_3S(CH_2)_3S(CH_2)_3SCH_2Ph]PF_6$ crystallized in the orthorhombic space group *Pnma* with $a = 13.540(2)$ Å, $b = 12.774(3)$ Å, $c = 16.873(3)$ Å, $Z = 4$, $R = 0.039$ and $R_w = 0.047$.

Introduction

Rhodium-105 was proposed as a therapeutic radionuclide by Troutner about a decade ago.[1] Its nuclear properties and the kinetic inertness of d^6 Rh(III) complexes make ^{105}Rh very attractive as a therapeutic radionuclide. ^{105}Rh is a moderate energy β emitter (E_β(max) = 0.560 MeV (70%), 0.250 MeV (30%)) with a 36 h half-life, and it is available in "no carrier added" concentrations (i.e., virtually all Rh atoms are ^{105}Rh). In addition, ^{105}Rh emits a low abundance of imageable γ-rays (E_γ = 306 keV (5%), 319 keV (19%)) which would allow *in vivo* tracking of the therapeutic dose. Our research efforts are focused on developing Rh(III) complexes containing tetradentate ligands which can be formed in high yield (>90% yield) under relatively mild conditions using ^{105}Rh. These ligands will ultimately serve as bifunctional chelates to which a targeting molecule is appended (e.g., peptide, monoclonal antibody fragment, etc.) to direct the complex to its *in vivo* site of action. The 36 h half-life of ^{105}Rh makes it preferable to conjugate the biomolecule to the bifunctional chelate prior to complexation with ^{105}Rh, which requires mild synthetic conditions.

Research efforts in developing potential radiopharmaceuticals based on ^{105}Rh have focused primarily on Rh(III) complexes with N and O donor ligands, such as amine oxime[2,3] amine−phenol,[4] amine,[5,6] and porphyrin[7] ligands. Although these ligand systems appear to form stable, kinetically inert complexes with ^{105}Rh, the reaction conditions needed to obtain ~95% complexation yield were fairly harsh (2 h reflux in aqueous ethanol) and often such high yields were not observed.[2,6,7] Recently, several reports have shown that Rh(III) forms very stable and kinetically inert complexes with crown thioethers.[8−14] Blake et al.[8,9] synthesized and characterized Rh(III) complexes with 12-, 14-, and 16-membered tetrathiamacrocycles ([12]-, [14]-, and [16]aneS_4) and reported that Rh(III) forms only *cis* complexes with the two smaller ring sizes and exclusively the *trans* isomer with the 16-membered S_4 macrocycle. The high stability of macrocyclic thioether Rh(III) complexes is attributed to a combination of the macrocyclic effect and the π-acidity of the sulfur atoms. The configurational isomerism of the Rh(III) complexes with the macrocyclic ligands was found to be a function of ring size and flexibility of the macrocyclic ring. We recently reported on the chemistry of ^{105}Rh complexed with a [16]aneS_4-diol macrocycle[11] and demonstrated its stability *in vitro* for greater than 5 days in pH 7.4 phosphate buffer and human serum, and Li et al.[15] discussed the pharmacokinetics of ^{105}Rh complexes with tetradentate amine−thioether ligands.

* Author to whom correspondence should be addressed.
† University of Missouri.
‡ Paul Scherrer Institut.
⊗ Abstract published in *Advance ACS Abstracts,* December 1, 1996.

(1) Grazman, B.; Troutner, D. E. *Appl. Radiat. Isot.* **1988**, *39*, 257.
(2) Siripaisarnpipat, S.; Schlemper, E. O. *Inorg. Chem.* **1984**, *23*, 330.
(3) Efe, E. G.; Pillai, M. R. A.; Schlemper, E. O.; Troutner, D. E. *Polyhedron* **1991**, *10*, 1617.
(4) Pillai, M. R. A.; John, C. S.; Troutner, D. E. *Bioconjugate Chem.* **1990**, *2*, 191.
(5) Pillai, M. R. A.; Lo, J. M.; John, C. S.; Troutner, D. E. *Nucl. Med. Biol.* **1990**, *17*, 419.
(6) Kruper, W. J., Jr.; Pollock, D. K.; Fordyce, W. A.; Fazio, M. J.; Inbasekaram, M. N. US Patent 4,994,560, February 19, 1991.
(7) Pillai, M. R. A.; Lo, J. M.; Troutner, D. E. *Appl. Radiat. Isot.* **1990**, *41*, 69.
(8) Blake, A. J.; Reid, G.; Schröder, M. *J. Chem. Soc., Dalton Trans.* **1989**, 1675.
(9) Blake, A. J.; Reid, G.; Schröder, M. *Polyhedron* **1992**, *11*, 2501.
(10) Cooper, S. R. *Acc. Chem. Res.* **1988**, *21*, 141.
(11) Venkatesh, M.; Goswami, N.; Volkert, W. A.; Schlemper, E. O.; Ketring, A. R.; Barnes, C. L.; Jurisson, S. *Nucl. Med. Biol.* **1996**, *23*, 33.
(12) Blake, A. J.; Reid, G.; Schröder, M. *Polyhedron* **1990**, *9*, 2925.
(13) Collison, D.; Reid, G.; Schröder, M. *Polyhedron* **1992**, *11*, 3165.
(14) Blake, A. J.; Holder, A. J.; Hyde, T. I.; Kuppers, H.; Schröder, M.; Stotzel, S.; Wieghardt, K. *J. Chem. Soc., Chem. Commun.* **1989**, 1600.
(15) Li, N.; Ochrymowycz, L. A.; Higginbotham, C.; Struttman, M.; Abrams, M. J.; Vollano, J. F.; Skerlj, R. T.; Ketring, A. R.; Volkert, W. A. *J. Labelled Compd Radiopharm.* **1995**, *37*, 426.

S0020-1669(96)00952-4 CCC: $12.00

Chart 1. Structures and Acronyms for the Tetrathioether Ligands

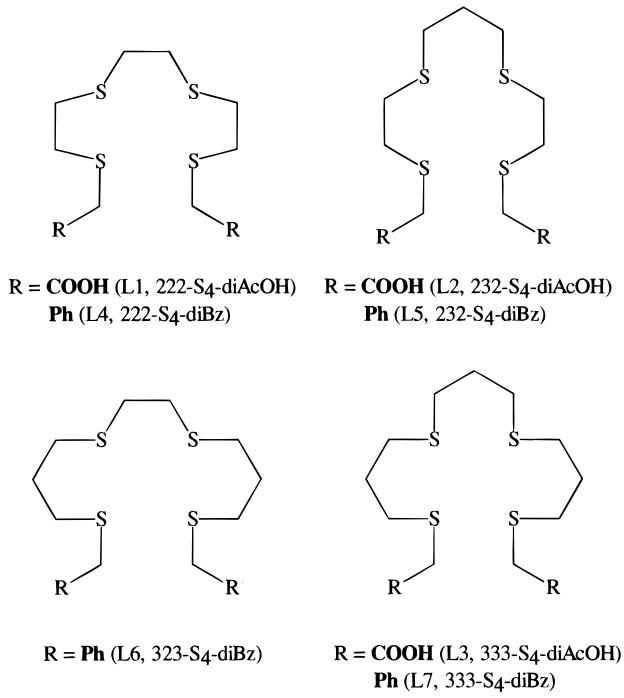

It should be pointed out that under "no carrier added" ^{105}Rh complexation conditions, the starting compound is a mixture of primarily anionic Rh(III)-105−chloride species[11] and that at least 10% by volume of ethanol is required to achieve high complexation yields.[11,15] The ethanol presumably reduces small quantities of the Rh(III) to Rh(I) to facilitate the substitution reaction, and then atmospheric oxygen reoxidizes the Rh(I) to generate the kinetically inert Rh(III) complex.[16−19] This method allows "no carrier added" Rh(III)-105 complexes with thioether ligands to be efficiently formed in aqueous solution under slightly acidic conditions (pH 4−7).[11,15]

We have extended our work with tetradentate thioether ligands to the related acyclic analogs. Our aims were to clearly understand the similarities and differences (in terms of structure, stereochemistry and stability of the complexes) between the macrocyclic and the related acyclic tetrathioether ligands in complexing Rh(III) and to evaluate these open chain ligands in the development of new radiopharmaceuticals based on ^{105}Rh. We have investigated the ligand systems **L1**−**L7** (Chart 1). These acyclic S_4-tetrathioethers differ in their backbone chain lengths and the identities of their terminal R groups. The backbone variations allowed us to probe the effect of chain length on the configuration of the sulfur atoms about the Rh, both with regard to *cis*/*trans* isomerization and to the orientation of the sulfur atoms themselves (i.e., *R*/*S*). The pendant R groups allow fine tuning of the properties of the resultant complex and incorporation of a functional group for conjugation to a biotargeting moiety. Here we report the synthesis of the open chain S_4 ligands, their complex formation with Rh(III), and characterization by spectroscopic (UV−vis, FT-IR and NMR) and single-crystal X-ray diffraction analysis techniques. The Rh(III) complexes formed with **L1**, **L2**, and **L3**, which contain two free carboxylic acid groups each, are of particular interest for extension to the radiotracer ^{105}Rh level for potential application to radiotherapy. However, difficulty in obtaining X-ray quality crystals for assignment of stereochemistry necessitated the synthesis of the dibenzyl-S_4 analogs. Full characterization of the Rh(III) complexes with the dibenzyl-S_4 ligands (**L4**−**L7**) allowed assignment of the conformations of the dicarboxylic acid-S_4−Rh(III) complexes based on comparisons of their spectroscopic characterizations. Our discussions focus on some interesting differences between the configurational isomerism observed for macrocyclic and acyclic tetrathioether Rh(III) complexes. The solid state X-ray crystal structures of the rhodium complexes are compared to their solution structures as determined by 1D and 2D NMR and electronic absorption spectroscopy.

Chart 2. Synthesis of the Acyclic S_4-diBz Ligands[a]

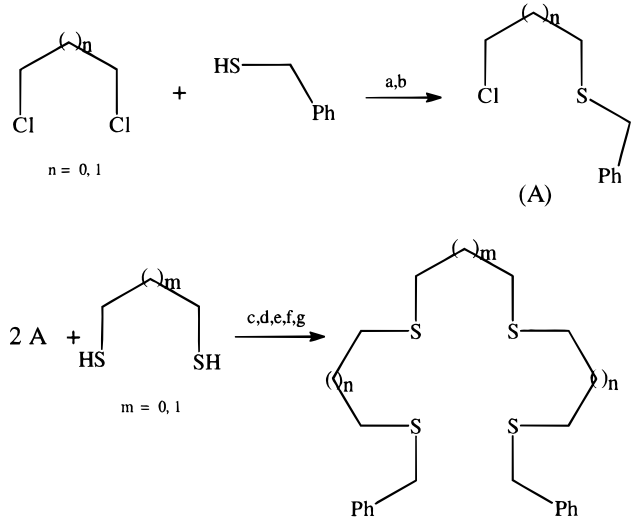

[a] Key: (a) triethylamine, N_2, reflux 6 h; (b) filter, vacuum distill (0.2 mbar, 100 °C); (c) NaOEt, N_2, reflux 2 h; (d) filter, remove solvent; (e) wash with hexane; (f) precipitate at −50 °C, wash with hexane; (g) recrystallize from Et_2O.

Experimental Section

Reagents and Materials. The chemicals required for the synthesis of ligands 1,12-diphenyl-2,5,8,11-tetrathiadodecane (**L4**, 222-S_4-diBz), 1,13-diphenyl-2,5,9,12-tetrathiatridecane (**L5**, 232-S_4-diBz), 1,14-diphenyl-2,6,9,13-tetrathiatetradecane (**L6**, 323-S_4-diBz), and 1,15-diphenyl-2,6,10,14-tetrathiapentadecane (**L7**, 333-S_4-diBz) were purchased from Aldrich Chemical Co. Rhodium trichloride (trihydrate) was obtained either from Aldrich Chemical Co. or from Acros Chemicals. All chemicals were of reagent grade and used as received unless otherwise specified.

2,5,8,11-Tetrathiadodecane-1,12-dicarboxylic acid (**L1**, 222-S_4-diAcOH), 2,5,9,12-tetrathiatridecane-1,13-dicarboxylic acid (**L2**, 232-S_4-diAcOH), and 2,6,10,14-tetrathiapentadecane-1,15-dicarboxylic acid (**L3**, 333-S_4-diAcOH) were available from a previous study.[20]

Benzylmercaptoethyl Chloride ($PhCH_2S(CH)_2Cl$) (Intermediate 1). ***Caution!*** *Intermediate 1 is a potential alkylating agent and appropriate care should be taken while handling this reagent*. The general synthetic scheme of the intermediates and ligands **L4**−**L7** is shown in Chart 2. Benzyl mercaptan (4.96 g, 0.040 mol) was added to excess 1,2-dichloroethane (39.6 g, 0.40 mol) and dry triethylamine (4 mL, 0.050 mol) in a 3-necked round-bottom flask purged with N_2. The reaction mixture was refluxed for 6 h under N_2. During this time a white precipitate (triethylamine hydrochloride) formed. The reaction mixture was cooled to room temperature and the precipitate removed by filtration. The excess 1,2-dichloroethane was removed under vacuum at <60 °C. The oily intermediate benzylmercaptoethyl chloride was purified by vacuum distillation (100 °C and 0.1 mbar) and characterized by NMR spectroscopy. Yield: 4.5 g (60%). $\rho = 1.15$

(16) Basolo, F.; Pearson, R. G. *Mechanisms of Inorganic Reactions*; Wiley: New York, 1967.
(17) Gillard, R. D.; Wilkinson, G. *J. Chem. Soc.* **1964**, 1224.
(18) Rund, J. V.; Basolo, F.; Pearson, R. G. *Inorg. Chem.* **1964**, *3*, 658.
(19) Addison, A. W.; Guillard, R. D.; Vaughan, H. *J. Chem. Soc., Dalton Trans.* **1973**, 1187.
(20) Nef, W. Ph.D. Thesis, University of Basel, 1996.

Table 1. Crystal Data, Data Collection Parameters, and Refinement Parameters[a]

	cis-[$RhCl_2$(222-S_4-dibz)]PF_6	*trans*-[$RhCl_2$(232-S_4-dibz)]PF_6	*trans*-[$RhCl_2$(323-S_4-dibz)]PF_6	*trans*-[$RhCl_2$(333-S_4-dibz)]PF_6
formula	$RhC_{20}H_{26}S_4Cl_2^+ PF_6^-$	$RhC_{21}H_{28}S_4Cl_2^+ PF_6^-$	$RhC_{22}H_{30}S_4Cl_2^+ PF_6^-$	$RhC_{23}H_{32}S_4Cl_2^+ PF_6^-$
fw	713.43	727.46	741.49	755.51
space group	$P2_1/c$	$P2_1/c$	$P\bar{1}$	*Pnma*
a, Å	14.365(2)	10.937(3)	7.732(2)	13.540(2)
b, Å	13.200(3)	19.055(2)	13.046(3)	12.774(3)
c, Å	15.736(2)	13.734(4)	15.720(2)	16.873(3)
α, deg			67.62(2)	
β, deg	115.571(4)	103.596(13)	79.63(2)	
γ, deg			78.60(2)	
V, Å^3	2691.6(8)	2782(1)	1427.7(6)	2918(1)
Z	4	4	2	4
ρ_{calc}, g/cm^3	1.761	1.737	1.725	1.720
T, °C	23	23	23	23
μ, cm^{-1}	12.3	11.9	11.7	11.4
λ source, Å	0.70930	0.70930	0.70930	0.70930
R	0.048	0.037	0.049	0.039
R_w	0.057	0.046	0.061	0.047

[a] Least-squares weights, $w = \sigma^{-2}(F_o)$, were calculated with the assumption that $\sigma^2 = \epsilon^2 + (\rho\iota)^2$ where ϵ is the statistical counting error and $\rho = 0.04$. The function minimized in the least-squares refinements were $\sum w(|F_o| - |F_c|)^2$. *R* is defined as $\sum||F_o| - |F_c||/\sum|F_o|$ while $R_w = [\sum w(|F_o| - |F_c|)^2/\sum w|F_o|^2]^{1/2}$.

g/mL. ^{1}H NMR ($CDCl_3$): δ(ppm) 2.75 (m, S***CH*****$_2$**), 3.55 (m, Cl***CH*****$_2$**), 3.75 (s, Ph***CH*****$_2$**), 7.20−7.45 (m, ***C*****$_6$*****H*****$_5$**).

1,12-Diphenyl-2,5,8,11-tetrathiadodecane (L4). Benzylmercaptoethyl chloride (3.25 mL, 0.020 mol) was added to 1,2-ethanedithiol (0.83 mL, 0.010 mol) and triethylamine (2.8 mL, 0.020 mol) in a round-bottom flask, and the resultant mixture was refluxed under N_2 for 3 h. The reaction mixture was cooled to room temperature and slurried with 100 mL of diethyl ether, and the solid triethylamine hydrochloride was removed by filtration. After the solvent was removed under vacuum, the oily residue was washed several times with hexane at ca. −50 °C. The remaining solid was recrystallized from diethyl ether, collected by filtration, and dried under vacuum (2.36 g, 60% yield): mp 30 °C. ^{1}H NMR (CD_3CN): δ (ppm) 2.58−2.64 (m, S***CH*****$_2$**), 3.75 (s, Ph***CH*****$_2$**), 7.23−7.32 (m, ***C*****$_6$*****H*****$_5$**).

Benzylmercaptopropyl Chloride (Intermediate 2). ***Caution!*** *Intermediate 2 is a potential alkylating agent and appropriate care should be taken while handling this reagent.* Benzylmercaptopropyl chloride was prepared using the method described above for the synthesis of intermediate **1**. The product was purified by vacuum distillation (130 °C, 0.2 mbar) and was characterized by NMR spectroscopy. Yield: 5.21 g (65%). ρ = 1.21 g/mL. ^{1}H NMR ($CDCl_3$): δ (ppm) 1.90−2.20 (m, CH_2***CH*****$_2$**CH_2), 2.65 (t, S***CH*****$_2$**, J = 8.3 Hz), 3.65 (t, ***CH*****$_2$**Cl, J = 8.7 Hz), 3.85 (s, Ph***CH*****$_2$**), 7.20−7.40 (m, ***C*****$_6$*****H*****$_5$**).

1,13-Diphenyl-2,5,9,12-tetrathiatridecane (L5), 1,14-Diphenyl-2,6,9,13-tetrathiatetradecane (L6), and 1,15-Diphenyl-2,6,10,14-tetrathiapentadecane (L7). In each preparation the appropriate benzylmercaptoalkyl chloride intermediate (0.0200 mol) was added to either 1,2-ethanedithiol or 1,3-propanedithiol (0.0100 mol) and freshly prepared sodium ethoxide (made by dissolving 1.15 g (0.05 mol) of Na in 20 mL of absolute ethanol) in a 3-necked round-bottom flask. The resultant mixture was refluxed for 5−6 h under N_2 atmosphere. Silica gel TLC was used to monitor the reaction for completion, and additions of the two reactants were made as necessary. After the reaction was cooled to room temperature and diethyl ether (20 mL) added, the sodium chloride was removed by filtration. The solvent was removed under vacuum, and then the crude products were repeatedly extracted with hexane, leaving an oily residue. The products were recrystallized from 50/50 (v/v) diethyl ether/hexane at ca. −50 °C and dried in vacuum, yielding oils at room temperature (90−95% yield).

Synthesis of Rh(III) Complexes. All Rh(III) complexes were prepared using a common procedure. $RhCl_3 \cdot 3H_2O$ (80 mg, 0.30 mmol) dissolved in 2 mL of acetonitrile at ca. 85 °C was added dropwise to a refluxing solution of the ligand (0.29 mmol) in 50 mL of a 4% (v/v) acetonitrile/ethanol solution. The reaction mixture was refluxed for 1 h, the development of a bright yellow color indicating complex formation. After filtration to remove insolubles, an excess of solid NH_4PF_6 or $NaBPh_4$ was added with stirring, resulting in a yellow precipitate for all complexes except **L2** and **L3**. For these two ligands the products were recovered as the Cl^- salts on removing the solvent by rotary evaporation. All the products (Cl^-, PF_6^-, or BPh_4^- salts) were recrystallized from acetonitrile/ethanol (50/50 v/v), washed with hexane and diethyl ether, and dried in vacuo with yields in the 40−80% range.

***cis*-[RhCl$_2$L1]PF$_6$.** Yield: 87 mg (43%). Anal. Found (calcd for $RhC_{10}Cl_2S_4H_{18}O_4PF_6 \cdot C_2H_5OH$): C, 20.67 (20.70); H, 3.42 (3.45); Cl, 9.72 (10.20); S, 18.57 (18.42).

***cis*/*trans*-[RhCl$_2$L2]Cl.** Yield: 87 mg (54%).

***trans*-[RhCl$_2$L3]Cl.** Yield: 90 mg (50%). Anal. Found (calcd for $RhC_{13}Cl_3S_4H_{24}O_4 \cdot C_2H_5OH$): C, 27.80 (28.68); H, 4.14 (4.78); Cl, 15.44 (16.10); S, 20.17 (20.39).

***cis*-[RhCl$_2$L4]PF$_6$.** Yield: 165 mg (80%). Anal. Found (calcd for $RhC_{20}Cl_2S_4H_{26}PF_6$): C, 33.34 (33.67); H, 3.46 (3.67); Cl, 9.33 (9.93); S, 18.54 (17.98).

***cis*/*trans*-[RhCl$_2$L5]PF$_6$.** Yield: 158 mg (75%). Anal. Found (calcd for $RhC_{21}Cl_2S_4H_{28}PF_6$): C, 34.78 (34.67); H, 3.73 (3.84); Cl, 9.86 (9.75); S, 17.78 (17.63).

***trans*-[RhCl$_2$L6]PF$_6$.** Yield: 107.4 mg (50%). Anal. Found (calcd for $RhC_{22}Cl_2S_4H_{30}PF_6$): C, 34.88 (35.68); H, 3.75 (4.00); Cl, 9.86 (9.58), S, 17.55 (17.32).

***trans*-[RhCl$_2$L7]PF$_6$.** Yield: 120.4 mg (55%). Anal. Found (calcd for $RhC_{23}Cl_2S_4H_{32}PF_6$): C, 35.02 (36.66); H, 3.95 (4.20); Cl, 10.45 (9.41); S, 16.48 (17.02).

Physical Measurements. UV−visible spectra were obtained in acetonitrile using a Hewlett-Packard HP 8452A diode array spectrophotometer. Infrared spectra were obtained as CsI pellets on a Nicolet 20DXB FT-IR spectrometer. ^{1}H- and ^{13}C-NMR were recorded in acetonitrile-d_3 (unless otherwise indicated) using a Bruker ARX-250 spectrometer. The ^{13}C spectra were obtained in the proton decoupled mode. Elemental analyses were performed by Quantitative Technologies, Inc., Whitehouse, NJ.

X-ray Diffraction Analysis. Yellow crystals of the PF_6^- salts of *cis*-[$RhCl_2$**L4**]$^+$, *trans*-[$RhCl_2$**L5**]$^+$, *trans*-[$RhCl_2$**L6**]$^+$, and *trans*-[$RhCl_2$**L7**]$^+$ were obtained as described above. Intensity data were obtained on an Enraf-Nonius CAD 4 automatic diffractometer, using the $\omega-2\theta$ scan mode with Mo Kα radiation from a graphite monochromator (λ = 0.709 30 Å). Intensities were corrected for Lorentz and polarization effects. Equivalent reflections were merged, and semiempirical absorption corrections were made using the Ψ-scan technique. Space group, lattice parameters, and other relevant information are given in Table 1. The structures were solved by direct methods with full-matrix least-squares refinement, employing the NRCVAX package.[21−26] All non-hydrogen atoms were refined with anisotropic

(21) Gabe, E. J.; Le Page, Y.; Charland, J.-P.; Lee, F. L.; White, P. S. *J. Appl. Crystallogr.* **1989**, *22*, 384−387.
(22) Flack, H. *Acta Crystallogr.* **1983**, *A39*, 876.
(23) Scattering factors, including *f′* and *f″*, were taken from: *International Tables for Crystallography*; Kynoch Press: Birmingham, England, 1974; Vol. IV.

Table 2. Electronic Absorbance Spectra for $[RhCl_2(S_4)]X$ in CH_3CN

complex	d−d transitions[a]	charge transfer transitions[a]
cis-$[RhCl_2$**L1**$]PF_6$	388 (1010), 298 (4090)	238 (19 060)
cis/*trans*-$[RhCl_2$**L2**$]Cl$	426 (681), 370 (1680)	256 (12 000), 210 (16 000)
trans-$[RhCl_2$**L3**$]Cl$	442 (330), 338 (1605)	256 (9310), 210 (17 000)
cis-$[RhCl_2$**L4**$]PF_6$	386 (1120), 294 (3560)	226 (18 000), 208 (20 100)
cis/*trans*-$[RhCl_2$**L5**$]PF_6$	426 (708), 360 (1800)	266 (15 000), 204 (16 500)
trans-$[RhCl_2$**L6**$]PF_6$	436 (330), 338 (1500)	270 (17 000), 222 (17 100), 204 (18 000)
trans-$[RhCl_2$**L7**$]PF_6$	440 (159), 336 (1550)	288 (16 700), 220 (13 000), 205 (19 100)

[a] λ in nm, ϵ in M^{-1} cm^{-1}.

thermal parameters. The hydrogen atoms were placed at calculated positions and included in the refinement using a riding model, with fixed isotropic *U*. The absolute configurations of the structures were determined by refinement of the η parameter.[27] The final difference maps had no features of chemical significance.

Results and Discussion

The structures, conformations and numbers of isomers formed for the Rh(III) complexes with the dicarboxylic acid−tetrathioether ligands (**L1**−**L3**) were of interest because it is particularly important that any potential radiopharmaceutical consist of only a single product (and a single isomer). The complete characterization, including X-ray crystal structures, of the complexes with the dibenzyl−tetrathioether ligands (**L4**−**L7**) allowed assignment of the dicarboxylic acid analogs by comparisons of their spectroscopic properties.

Synthesis. The Rh(III) complexes with the ligands **L1**−**L7** were synthesized by a common procedure (*vide infra*) which was similar to that reported by Blake.[8] Fairly low concentrations of the reactants were used to maximize yield and avoid formation of insoluble rhodium hydroxy compounds.[28,29] All complexes were air-stable and easy to handle at room temperature. $[RhCl_2(232\text{-}S_4\text{-diAcOH})]Cl$ proved very difficult to isolate sufficiently pure for elemental analysis. This was in part due to the presence of multiple isomers (*vide infra*). For this reason, only NMR and FT-IR analyses were obtained.

Electronic Absorption and Far-Infrared Spectroscopy. The UV−visible absorption spectra (Table 2) of each of the Rh(III) complexes gave characteristic transitions in the range 200−500 nm. The two spin-allowed d−d transition bands ($^1T_{1g} \leftarrow {}^1A_{1g}$, and $^1T_{2g} \leftarrow {}^1A_{1g}$) were observed in the range 280−500 nm with charge transfer bands observed below 280 nm. The intensity of the d−d transitions in the $[RhCl_2S_4]^+$ complexes has been found characteristic for their geometry, with the lower symmetry *cis*-dichloro complexes exhibiting significantly larger molar extinction coefficients than the *trans*-dichloro complexes.[8,30,31] In addition, the position of the d−d bands was found to be characteristic for the geometry of these complexes, although this was not the case for the macrocyclic tetrathioether complexes previously reported.[8,11] The lower energy d−d transitions were observed between 385 and 390 nm for the *cis* complexes while those for the *trans* complexes were observed between 435 and 445 nm. Likewise, the higher energy d−d transitions were observed between 290 and 295 nm for the *cis* complexes and between 335 nm and 340 nm for the *trans* complexes. The complexes $[RhCl_2$**L1**$]^+$ and $[RhCl_2$**L4**$]^+$ were assigned as having the *cis* configuration based on the intensity of the lower energy d−d transition band (e.g., $\epsilon_{388} = 1010$ M^{-1} cm^{-1} for *cis*-$[RhCl_2$**L1**$]^+$ and $\epsilon_{386} = 1120$ M^{-1} cm^{-1} for *cis*-$[RhCl_2$**L4**$]^+$). Although the higher energy d−d band was also indicative of *cis*/*trans* isomerization, it was occasionally observed as a shoulder on a charge transfer band and thus not as reliable. Likewise, $[RhCl_2$**L3**$]^+$, $[RhCl_2$**L6**$]^+$, and $[RhCl_2$**L7**$]^+$ were assigned as *trans*-dichloro rhodium complexes based on the observed molar extinction coefficients of the d−d transition bands (ϵ (M^{-1} cm^{-1}) = 330, 330, and 159, respectively). The complexes $[RhCl_2$**L2**$]^+$ and $[RhCl_2$**L5**$]^+$ were isolated as mixtures of the *cis* and *trans* isomers as indicated by their ^{13}C NMR spectra (*vide infra*).

Table 3. Selected Far-IR Spectral Bands

complex	ν(Rh−Cl) in cm^{-1}
cis-$[RhCl_2$**L1**$]PF_6$	336, 304
cis/*trans*-$[RhCl_2$**L2**$]PF_6$	371, 357, 325, 305
trans-$[RhCl_2$**L3**$]PF_6$	382
cis-$[RhCl_2$**L4**$]PF_6$	346, 314
cis/*trans*-$[RhCl_2$**L5**$]PF_6$	352, 336, 328, 301
trans-$[RhCl_2$**L6**$]PF_6$	370
trans-$[RhCl_2$**L7**$]PF_6$	317

The far-IR bands (Table 3) for ν(Rh−Cl) obtained in a CsI matrix (in the range 250−400 cm^{-1}) for each of the complexes were consistent with the assignment as the *cis* or *trans* isomer.[32] Two sharp IR bands of ν(Rh−Cl) were observed in the range 300−400 cm^{-1} for each of the *cis* complexes, and one sharp band was observed for each of the *trans* complexes consistent with symmetry-allowed vibrations. Four IR bands were observed for $[RhCl_2$**L2**$]^+$ and $[RhCl_2$**L5**$]^+$ in the 300−400 cm^{-1} range, probably from the presence of multiple *cis* and *trans* isomers in the mixture.

NMR Spectroscopy of the Rh(III) Complexes. The ^1H NMR spectral data of the ligands and their Rh(III) complexes are given in Table 4. The ^1H NMR spectra of the complexes were consistent with the proposed formulations; however, the complexity of the spectra due to the conformations and coupling with Rh-103 (spin $^1/_2$) made interpretation difficult. The phenyl protons of the BPh_4^- counterions were used as an internal integration reference and confirmed that the complexes were +1 cations.

^{13}C NMR spectra were indicative of the number of isomers in solution (Table 5). For example, $[RhCl_2$**L1**$]^+$ and $[RhCl_2$**L4**$]^+$ each showed four CH_2 signals consistent with a single isomer. Both the acyclic **L1** and **L4** and its related macrocycle [12]-aneS_4 formed exclusively single *cis* dichloro isomers on complexation with Rh(III).[8] However, the larger (by one spacer CH_2 group) **L2** and **L5** yielded mixtures of *cis* and *trans* dichloro isomers as evidenced by their ^{13}C NMR spectrum (Table 5). On the basis of the number of signals for the central carbon of the propylene group of **L2** and **L5**, it appears as if three isomers were formed on complexation. Their relative intensities were approximately 2:1:1; however, nothing more can be said regarding their identities at this time. Blake[8] isolated

(24) Larson, A. C. *Crystallographic Computing*; Munksgaard: Copenhagen, 1970; p 293.
(25) Le Page, Y. *J. Appl. Crystallogr.* **1988**, *21*, 983.
(26) Le Page, Y.; Gabe, E. J. *J. Appl. Crystallogr.* **1979**, *12*, 464.
(27) Rogers, D. *Acta Crystallogr.* **1981**, *A37*, 734−741.
(28) Cervini, R.; Fallon, G. D.; Spiccia, L. *Inorg. Chem.* **1991**, *30*, 831.
(29) Read, M. C.; Glaser, J.; Sandstrom, M.; Toth, I. *Inorg. Chem.* **1992**, *31*, 4155.
(30) Bounsall, E. J.; Koprich, S. R. *Can. J. Chem.* **1970**, *48*, 1481.
(31) Sokol, L. S. W. L.; Ochrymowycz, L. A.; Rorabacher, D. B. *Inorg. Chem.* **1981**, *20*, 3189.
(32) Braunstein, P.; Chauvin, Y.; Nahring, J.; DeCian, A.; Fischer, J. *J. Chem. Soc., Dalton Trans.* **1995**, 863.

Table 4. ^{1}H NMR Data for the Free Ligands (**L1**−**L7**) and Their Rh(III) Complexes[a,b]

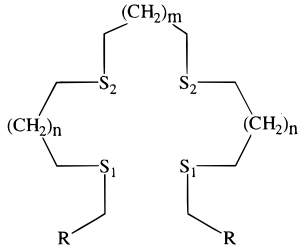

ligand	R	assignment	δ (ppm) of ligand	integration	assignment	δ (ppm) of $[RhCl_2L]PF_6$	integration
L1	COOH	S2***CH*$_2$*CH*$_2$S2	2.74 (s)	4	S2***CH*$_2$*CH*$_2$S2	2.70−2.90 (m), 3.42−3.60 (m)	2, 2
	$n, m = 0$	S1***CH*$_2$*CH*$_2$S2	2.78−2.84 (m)	8	S1***CH*$_2$*CH*$_2$S2	3.10−3.40 (m)	8
		***CH*$_2$COOH	3.67 (s)	4	***CH*$_2$COOH	4.10−4.30 (m)	4
L2[c]	COOH	S2CH$_2$***CH*$_2$CH$_2$	1.83 (p, $J = 7.17$)	2	**CH$_2$**	2.25−3.58 (m)	14
	$n = 0, m = 1$	***CH*$_2$S2***CH*$_2$	2.62 (t, $J = 7.17$)	4			
		S1***CH*$_2$CH$_2$	2.69−2.76 (m)	8			
		***CH*$_2$COOH	3.26 (s)	4	***CH*$_2$COOH	4.03−4.51 (m)	4
L3	COOH	S2CH$_2$***CH*$_2$CH$_2$	1.77−1.85 (m)	6	**CH$_2$**	2.20−3.84 (m)	18
	$n, m = 1$	***CH*$_2$S2***CH*$_2$	2.55−2.61 (m)	8			
		S1***CH*$_2$CH$_2$	2.66−2.72 (m)	4			
		***CH*$_2$COOH	3.22 (s)	4	***CH*$_2$COOH	4.02−4.55 (m)	4
L4	C_6H_5	S***CH*$_2$	2.58−2.64 (m)	12	S2***CH*$_2$*CH*$_2$S2	2.58−2.80 (m), 3.50−3.59 (m)	2, 2
	$n, m = 0$				S1***CH*$_2$*CH*$_2$S2	2.90−3.40 (m)	8
		***CH*$_2$C$_6$H$_5$	3.75 (s)	4	***CH*$_2$C$_6$H$_5$	4.45−4.65 (m)	4
		C$_6$H$_5$	7.23−7.32 (m)	10	**C$_6$H$_5$**	7.20−7.55 (m)	10
L5[c]	C_6H_5	S2CH$_2$***CH*$_2$CH$_2$	1.72 (p, $J = 7.17$)	2	**CH$_2$**	2.32−3.90 (m)	14
	$n = 0, m = 1$	S2***CH*$_2$CH$_2$CH$_2$	2.54 (t, $J = 7.17$)	4			
		S1***CH*$_2$*CH*$_2$S2	2.58−2.64 (m)	8			
		***CH*$_2$C$_6$H$_5$	3.76 (s)	4	***CH*$_2$C$_6$H$_5$	4.03−4.53 (m)	4
		C$_6$H$_5$	7.21−7.33 (m)	10	**C$_6$H$_5$**	7.20−7.60 (m)	10
L6	C_6H_5	S1CH$_2$***CH*$_2$CH$_2$S2	1.78 (p, $J = 7.15$)	4	S1CH$_2$***CH*$_2$CH$_2$S2	2.33−2.63 (m)	6
	$n = 1, m = 0$	S2***CH*$_2$CH$_2$CH$_2$	2.50 (t, $J = 7.15$)	4	S***CH*$_2$	3.07−3.60 (m)	12
		S1***CH*$_2$CH$_2$	2.57 (t, $J = 7.15$)	4			
		S2***CH*$_2$*CH*$_2$S2	2.65 (s)	4			
		***CH*$_2$C$_6$H$_5$	3.71 (s)	4	***CH*$_2$C$_6$H$_5$	3.75−4.75 (m)	4
		C$_6$H$_5$	7.21−7.32 (m)	10	**C$_6$H$_5$**	7.30−7.50 (m)	10
L7	C_6H_5	SCH$_2$***CH*$_2$CH$_2$S	1.72−1.80 (m)	6	**CH$_2$**	2.35−3.33 (m)	18
	$n, m = 1$	S***CH*$_2$	2.47−2.57 (m)	12			
		***CH*$_2$C$_6$H$_5$	3.71 (s)	4	***CH*$_2$C$_6$H$_5$	3.55−4.43 (m)	4
		C$_6$H$_5$	7.19−7.32 (m)	10	**C$_6$H$_5$**	7.21−7.40 (m)	10

[a] All spectra were obtained in CD_3CN. [b] The observed chemical shifts were designated as s = singlet, t = triplet, p = pentet, and m = multiplet. [c] A mixture of *cis* and *trans* $[RhCl_2$**L2**/**L5**$]PF_6$ isomers are formed, complicating the spectrum further.

Table 5. ^{13}C NMR Data for the Free Ligands (**L1**−**L7**) and their Rh(III) Complexes[a]

ligand	assignment	δ (ppm) of the free ligand	δ (ppm) of $[RhCl_2L]PF_6$
L1	aliphatic	32.11, 32.77, 33.33, 33.77	37.06, 39.10, 41.00, 42.12
	carboxylic	172.27	171.00
L2[b,c]	aliphatic	30.52, 31.15, 32.08, 33.28, 33.86	23.69, 23.80, 25.83, 29.84, 30.28, 31.32, 31.75, 32.15, 32.40, 32.62, 33.34, 33.51, 33.67, 34.52, 34.64, 35.41, 36.07, 36.51, 37.13, 37.34, 37.73, 37.99, 41.40, 41.78,42.10, 42.98
	carboxylic	172.08	167.56, 167.63, 167.99, 168.08, 168.18, 168.33, 168.36, 168.44, 168.52
L3[c]	aliphatic	29.81, 30.37, 31.15, 31.18, 32.00, 32.04, 34.50	21.95, 23.00, 29.75, 34.05, 35.10, 38.15
	carboxylic	172.16	171.20
L4[d]	aliphatic	31.26, 31.41, 31.79, 35.41	35.99, 36.99, 40.28, 40.95
	aromatic	126.89, 128.43, 128.81	128.95, 129.23, 130.09
L5[b,d]	aliphatic	30.50, 31.22, 32.28, 32.47, 36.52	23.83, 23.99, 25.92, 29.22, 29.96, 30.09, 30.22, 30.37, 30.48, 31.28, 32.51, 32.58, 34.21, 35.40, 35.99, 36.21, 37.60, 38.11, 38.38, 39.15, 39.55, 39.98, 40.30, 40.60, 41.92, 42.31
	aromatic	127.95, 129.49, 129.50	128.84, 129.04, 129.17, 130.16, 130.28, 130.60
L6[d]	aliphatic	29.12, 29.86, 30.25, 31.70, 35.54	23.28, 26.85, 30.60, 31.05, 36.59
	aromatic	126.77, 128.38, 128.78	128.57, 129.09, 129.78
L7[d]	aliphatic	29.04, 29.30, 29.88, 30.14, 30.18, 35.53	21.78, 22.24, 26.60, 32.46, 34.82, 36.82
	aromatic	126.77, 128.36, 128.78	128.60, 129.08, 129.89

[a] All spectra were obtained in CD_3CN. [b] A mixture of *cis* and *trans* $[RhCl_2$**L2**/**L5**$]PF_6$ isomers are formed giving rise to the numerous carbon signals for this complex. [c] The spectra of the Rh complexes with these ligands were obtained in DMSO-d_6 due to their low solubility in acetonitrile. [d] DEPT ^{13}C NMR were run.

exclusively the *cis* dichloro isomer with the related macrocycle [14]aneS_4. This difference may be attributed to a cavity size which is able to more easily expand in the acyclic ligands (*vide infra*).

The one-dimensional ^{1}H and ^{13}C NMR spectra of the analogous dibenzyl and dicarboxylic acid complexes indicated identical solution structures (Tables 4 and 5). Discounting the pendant carboxylic acid and benzyl functionalities, the spectra are identical. For example, the *cis* complexes with **L1** and **L4** both show their four methylene carbons between 35 and 43 ppm while the *trans* complexes with **L3** and **L7** exhibit six methylene carbons between 21 and 39 ppm (Table 5). The complexes with **L2** and **L5**, which each contain at least three isomers, exhibit analogous complexity in their spectra. An interesting

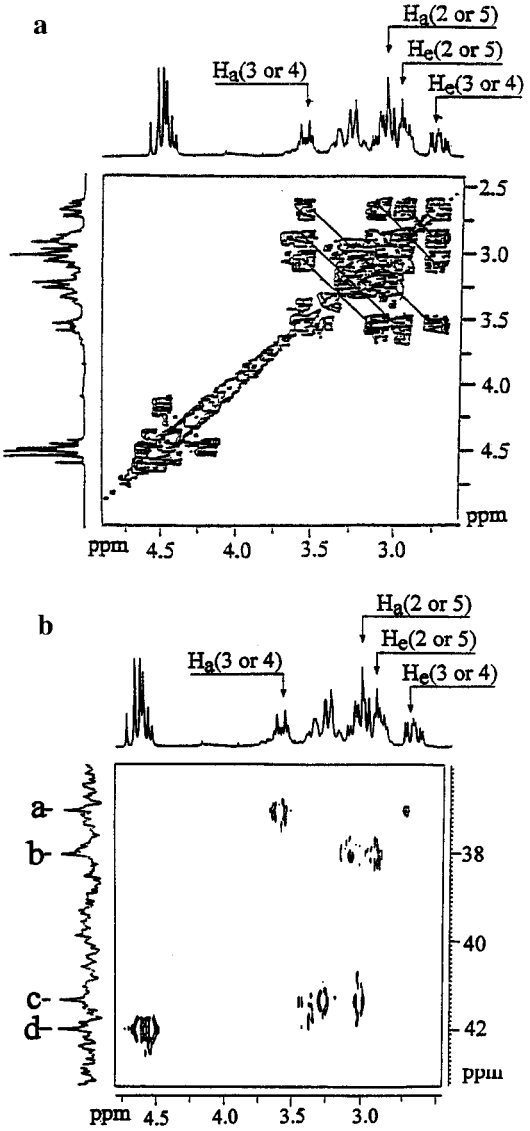

Figure 1. (a) 2D $^1H-^1H$ COSY NMR spectrum showing the aliphatic region for *cis*-[$RhCl_2$**L4**]BPh_4 (in CD_3CN). (b) 2D $^{13}C-^1H$ COSY NMR spectrum showing the aliphatic region for *cis*-[$RhCl_2$**L4**]BPh_4 (in CD_3CN): a = C(3 or 4), b = C(2 or 5), c = C(1 or 6), d = C(7 or 14).

observation is that the methylene C signals for the *trans* isomers occur further upfield than do similar resonances for the *cis* isomers.

Two features of particular interest were observed in the NMR spectra of the complexes: (a) the protons on the central ethylene bridge in **L1** and **L4** showed strong geminal coupling; (b) two aliphatic C signals for *trans*-[$RhCl_2$**L6**]PF_6 and three for *trans*-[$RhCl_2$**L3**]Cl and *trans*-[$RhCl_2$**L7**]PF_6 were observed significantly upfield from those in the corresponding ligand spectra. 2D NMR studies were performed for *cis*-[$RhCl_2$**L4**]PF_6, *trans*-[$RhCl_2$**L6**]PF_6, and *trans*-[$RhCl_2$**L7**]PF_6 to elucidate the solution structures that resulted in these spectral observations.

Two-dimensional $^1H-^1H$ and $^{13}C-^1H$ correlation spectra (COSY) for *cis*-[$RhCl_2$**L4**]$^+$ allowed assignment of multiplets at 3.61−3.42 ppm and 2.72−2.58 ppm to geminally coupled axial and equatorial protons on the equivalent C(3) and C(4) (see $^1H-^1H$ COSY spectrum, Figure 1a). These two pairs of protons (deshielded axial and shielded equatorial) are bonded to the most upfield shifted (36.94 ppm) central ethylene carbons as verified by the $^{13}C-^1H$ COSY spectrum (Figure 1b). The deshielding of the axial protons may be explained by through space electric field effects from the close proximity of the aromatic ring (see Figure 3 for the structure). This analysis is consistent with a solution structure analogous to that observed

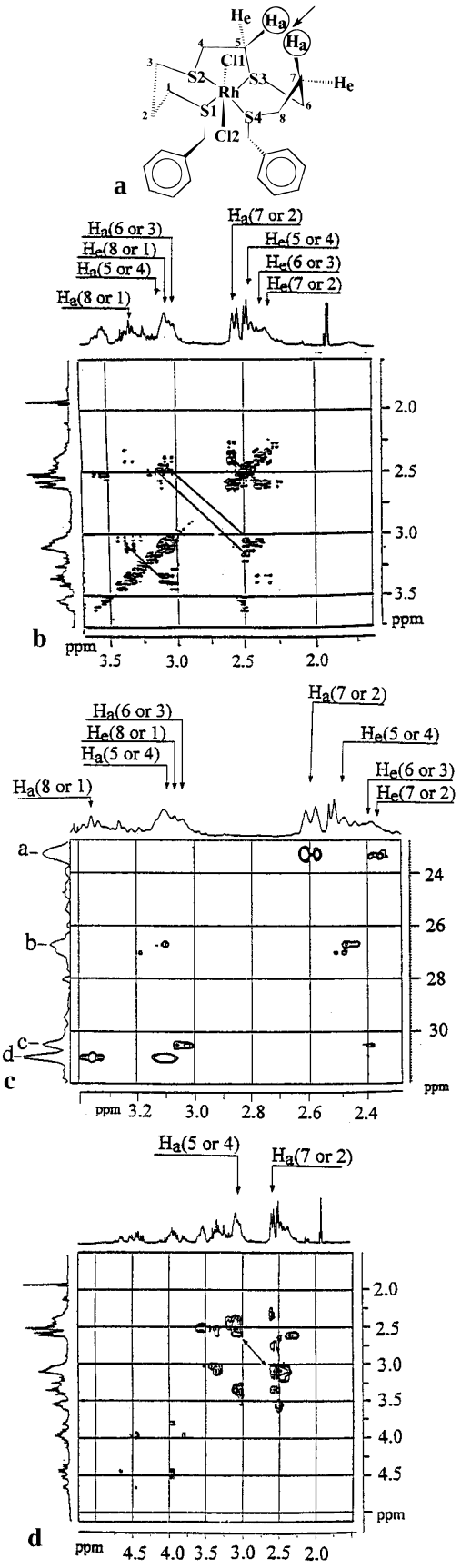

Figure 2. (a) Structural conformation of *cis*-[$RhCl_2$**L6**]$^+$. An arrow indicates the steric shielding effect between two closely spaced H atoms. (b) 2D $^1H-^1H$ COSY NMR spectrum showing the aliphatic region for *trans*-[$RhCl_2$**L6**]PF_6 (in CD_3CN). (c) 2D $^{13}C-^1H$ COSY NMR spectrum showing the aliphatic region for *trans*-[$RhCl_2$**L6**]PF_6 (in CD_3CN): a = C(7 or 2), b = C(5 or 4), c = C(6 or 3), d = C(8 or 1). (d) 2D $^1H-^1H$ NOESY NMR spectrum showing the aliphatic region for *trans*-[$RhCl_2$**L6**]PF_6 (in CD_3CN).

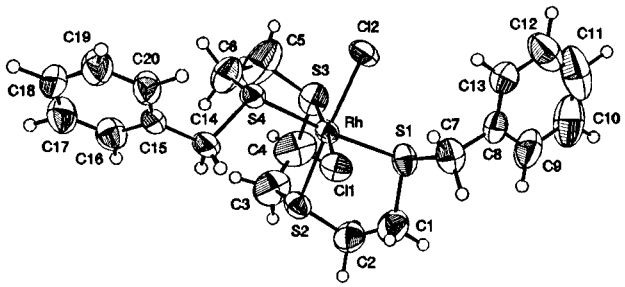

Figure 3. ORTEP representation (50% probability elipsoids) of *cis*-$[RhCl_2\mathbf{L4}]^+$.

in the solid state, which shows C(3) and C(4) very close in space to the phenyl moiety on S4 (Figure 3). Similar interactions are inferred for *cis*-$[RhCl_2\mathbf{L1}]^+$.

Two-dimensional $^1H-^1H$, $^{13}C-^1H$ (COSY), and $^1H-^1H$ NOESY NMR methods were used to elucidate the upfield shifting of the methylene C signals in the Rh(III) complexes with **L3**, **L6**, and **L7**. The positions of these resonances may be explained by steric interactions (1,4-diaxial) resulting from the close through space contact of the hydrogen atoms bonded to those carbon atoms.[33] The sterically induced polarization of the C−H bonds caused shielding of the carbon atoms resulting in the observed upfield shifts. The structural conformation of *trans*-$[RhCl_2\mathbf{L6}]^+$ as shown in Figure 2a illustrates the possible H−H steric interactions for $H_a(5)\cdots H_a(7)$. The equivalent interactions occur on the other side of the time averaged mirror plane and arise from the facile conformational flexibility of the six-membered chelate rings. The $^1H-^1H$ COSY spectrum of *trans*-$[RhCl_2\mathbf{L6}]^+$ indicated that the axial and the most upfield shifted equatorial protons (H_a 2.60 ppm, H_e 2.38 ppm) bonded to the most upfield carbon C(7) (23.28 ppm) were geminally coupled (see Figure 2b). Likewise, the axial H_a and equatorial H_e protons (3.10 and 2.42 ppm, respectively) bonded to the second most upfield carbon C(5) (26.85 ppm) were coupled, as indicated by the correlation cross peaks (Figure 2b). These *HH* connectivities were confirmed in the $^{13}C-^1H$ COSY spectrum (Figure 2c). The close contact of the hydrogen atoms C(7)−$H_a\cdots H_a$−C(5) (1,4 interaction) (Figure 2a) was confirmed by the 2D off-diagonal $^1H-^1H$ NOESY spectrum (Figure 2d) with the cross peaks at $\delta = 2.60$ ppm and $\delta = 3.10$ ppm. Analogous interactions were observed in the 2D NMR spectra for *trans*-$[RhCl_2\mathbf{L7}]^+$, showing coupling between the protons on C(5) and C(3) and between those on C(4) and C(2). The NMR spectra were consistent with the *trans* structure as determined by X-ray diffraction analysis.

X-ray Crystallography of Rh(III) Complexes. Single-crystal X-ray structures of the rhodium(III) complexes with the benzyl-substituted tetrathioether ligands (**L4**−**L7**) were determined in order to confirm the geometry and stereochemical features. These structure determinations allowed assignment of the configurations in the Rh(III) complexes prepared from the diacetic acid substituted tetrathioether analogs (**L1**−**L3**) based on spectroscopic information. Tables 1 and 6 list the experimental details and selected bond distances and angles, respectively, for the four structures.

Crystal Structure of *cis*-$[RhCl_2L4]PF_6$. An ORTEP[34] diagram of the cation *cis*-$[RhCl_2\mathbf{L4}]^+$ with its atomic numbering scheme is shown in Figure 3. The Rh^{III} ion is found to sit in a distorted octahedral environment, coordinating to four S atoms and two Cl atoms in a *cis* arrangement. The observed bond lengths and bond angles are similar to previously reported Rh(III)−S and Rh(III)−Cl bond distances.[8,11,35,36] The Rh−S2 (2.293(2) Å) and Rh−S3 (2.288(2) Å) bond lengths which are *trans* to chlorides are slightly shorter (ca. 0.05 Å) than the Rh−S1 (2.347(2) Å) and Rh−S4 (2.328(2) Å) bond lengths. This can be explained by π-back-bonding from the metal to the S atom. The *trans* Cl strengthens the back-bonding to the S through electron donation to the metal, however, the two *trans* S atoms compete for electron density from the metal.

Crystal Structure of *trans*-$[RhCl_2L5]PF_6$. Rh(III) formed a mixture of *cis* and *trans* isomers with ligand **L5**, and the *trans*-dichloro isomer was isolated as single crystals by slow evaporation from ethanol−acetonitrile solution. An ORTEP[34] diagram of the structure of the complex is shown in Figure 4. The Rh^{III} atom is positioned in the center of the S_4 cavity (endo position) of the complex in a slightly distorted octahedral geometry coordinating four S and two Cl atoms in the *trans* configuration. The bite angles involving the Rh and S atoms of the two five-membered chelating rings and one six-membered chelating ring are close to the ideal octahedral bond angles. A slightly larger deviation was observed in the open S1−Rh−S4 bond angle (94.47(5)°). This is accompanied by a lengthening in the Rh−S1 and Rh−S4 bonds (2.3774(1) and 2.360(2) Å, respectively) and may result from a combination of cavity size expansion to accommodate the large Rh(III) and the *trans* positioning of the two sterically crowding benzyl groups as depicted in Figure 4. The least-squares plane determination for the four S atoms shows them to be tetrahedrally distorted about the Rh atom which lies close to the mean plane with a deviation of 0.0308(9) Å. Each of the sulfur atoms deviated by an average of ±0.0761(24) Å from the plane. The reduced flexibility in the related macrocyclic tetrathioether ligand ([14]aneS_4) prevents Rh from bonding to the endo arrangement of the S_4 cavity, and so, exclusively, the *cis*-dichloro isomer is formed.

Crystal Structure of *trans*-$[RhCl_2L6]PF_6$. An ORTEP[34] representation of the structure of *trans*-$[RhCl_2\mathbf{L6}]^+$ with the atomic numbering scheme is displayed in Figure 5. Rh^{III} is coordinated by four equatorial S atoms and two axial Cl ions which are mutually *trans* to each other, and the coordination geometry around the metal ion is a distorted octahedron. One of the 6-membered chelate rings adopted a chair conformation (S1−Rh−S2, 86.41(8)°) while the other one exhibited a twist−boat conformation (S3−Rh−S4, 92.54(8)°) (Figure 5). The least-squares plane for the four S atoms showed them to be tetrahedrally distorted about the Rh atom. The Rh atom lies 0.0657(13) Å below the mean S_4 plane, with each of the S atoms deviating an average of ±0.133(4) Å. The two bulky benzyl groups orient themselves in *trans* positions. Significant deviation is found in the S−Rh−S bond angles as a result of the positioning of the benzyl groups (Table 6).

Crystal Structure of *trans*-$[RhCl_2L7]PF_6$. An ORTEP[34] view of this cation is shown in Figure 6. Only six-membered chelate rings are present in this complex, which would suggest greater conformational freedom with the larger cavity size of the ligand. Rh^{III} is found in the center of a distorted octahedron. The largest bond angle distortions were observed in this complex, with only the S1−Rh−S2 and its symmetry-related S3−Rh−S4 angles being close to the ideal 90°. The other angles had an average deviation from 90 deg of 7.55°. The structure of the related macrocyclic analog,[8,11] *trans*-$[RhCl_2(16ane S_4)]^+$, exhibited very close to ideal octahedral geometry with all angles within 1.1 deg of 90°. This suggests that the pendant benzyl groups may be responsible for the observed

(33) Breitmaier, E.; Voelter, W. *Carbon-13 NMR Sprectroscopy—High Resolution Methods and Applications in Organic Chemistry and Biochemistry*, 3rd ed.; VCH: Weinheim, Germany, 1990.
(34) Johnson, C. K. ORTEP—A Fortran Thermal Ellipsoid Plot Program. Technical Report ORNL-5138; ORNL: Oak Ridge, TN, 1976.
(35) Cooper, S. R.; Rawle, S. C.; Yagbasan, R.; Watkin, D. J. *J. Am. Chem. Soc.* **1991**, *113*, 1600.
(36) Brandt, K.; Sheldrick, W. S. *J. Chem. Soc., Dalton Trans.* **1996**, 1237.

Table 6. Selected Bond Distances (Å) and Angles (deg)

	cis-[$RhCl_2$(222-S_4-dibz)]PF_6	*trans*-[$RhCl_2$(232-S_4-dibz)]PF_6	*trans*-[$RhCl_2$(323-S_4-dibz)]PF_6	*trans*-[$RhCl_2$(333-S_4-dibz)]PF_6
Rh−S1	2.347(2)	2.377(1)	2.382(2)	2.373(2)
Rh−S2	2.293(2)	2.313(2)	2.322(2)	2.329(2)
Rh−S3	2.288(2)	2.310(2)	2.320(2)	2.329(2)
Rh−S4	2.328(2)	2.360(2)	2.362(2)	2.373(2)
Rh−Cl1	2.349(2)	2.339(1)	2.339(2)	2.335(2)
Rh−Cl2	2.366(2)	2.343(2)	2.347(2)	2.359(2)
S1−Rh−S2	87.55(7)	88.19(6)	86.41(8)	89.58(6)
S2−Rh−S3	89.86(9)	89.88(6)	87.93(8)	97.96(6)
S3−Rh−S4	88.68(8)	87.67(5)	92.54(8)	89.58(6)
S1−Rh−S4	174.27(7)	94.47(5)	93.69(7)	82.85(6)
S1−Rh−S3	92.92(8)	174.54(5)	173.12(8)	172.36(6)
S2−Rh−S4	97.96(7)	176.49(6)	170.35(8)	172.36(6)
S1−Rh−Cl1	91.49(8)	85.73(5)	90.57(7)	87.30(6)
S1−Rh−Cl2	88.87(7)	93.66(5)	90.84(8)	93.95(5)
S2−Rh−Cl1	89.05(7)	86.72(6)	95.61(8)	93.41(5)
S2−Rh−Cl2	175.76(8)	92.28(6)	83.82(8)	85.50(5)
S3−Rh−Cl1	175.40(8)	89.06(5)	86.09(8)	93.41(5)
S3−Rh−Cl2	88.04(9)	91.52(5)	92.43(8)	85.50(5)
S4−Rh−Cl1	87.05(7)	95.75(5)	94.03(7)	87.30(6)
S4−Rh−Cl2	85.68(7)	85.27(5)	86.53(8)	93.95(5)
Cl1−Rh−Cl2	93.33(8)	178.85(6)	178.44(8)	178.34(8)

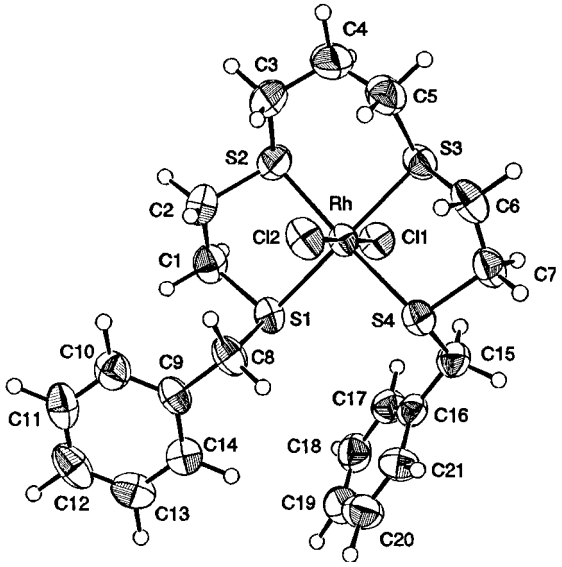

Figure 4. ORTEP representation (50% probability elipsoids) of *trans*-[$RhCl_2$**L5**]$^+$.

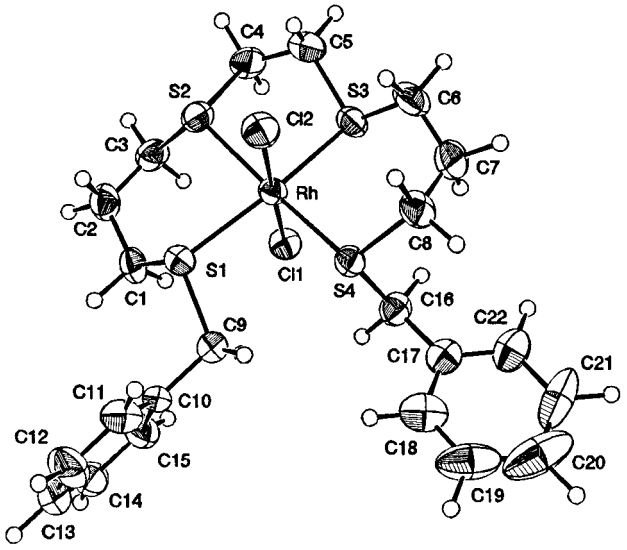

Figure 5. ORTEP representation (50% probability elipsoids) of *trans*-[$RhCl_2$**L6**]$^+$.

distortion in *trans*-[$RhCl_2$**L7**]$^+$. The four S atoms lie in the least-squares plane with the Rh atom lying 0.023(1) Å below it. The complex cation with its two opposite six-membered chelate rings in the boat conformation and the central ring in the chair conformation has C_s symmetry with its plane of symmetry passing through the Rh, both chlorides and C5.

Comparison of Structures of Acyclic and Macrocyclic Tetrathioether Metal Complexes. Macrocycles are more restricted in their bonding modes to metal ions by the reduced flexibility of the backbones between the coordinating atoms than are their related acyclic derivatives. The flexibility of the backbone affects the size of the cavity available for coordinating metal ions and impacts the bonding configuration of the ligand. This effect is demonstrated in the Rh(III) complexation with the acyclic ligand 232-S_4-diBz (**L5**), in which both *cis*- and *trans*-dichloro isomers are observed. The related macrocycle, [14]aneS_4, yielded only the *cis* isomer because Rh(III) is too large to be accommodated in the cavity. The complexes with the acyclic tetrathioether ligands exhibited both S−Rh−S bond angle and Rh−S bond length distortions. The three structures exhibiting the *trans*-dichloro configuration showed significant S−Rh−S bond angle variations compared to structures with the related macrocycles, although no large deviations from typical Rh−S bond distances were observed.[8,11,35,36] These effects were observed in the four S−Rh−S bond angles and in the S−S distances in these structures. Figure 7 illustrates these distortions for the related macrocyclic and acyclic tetrathioether complexes. Although it is difficult to say which backbone length is an appropriate match for the open end, [14]aneS_4 was considered for our purposes as the macrocyclic analog for both 232-S_4-diBz (**L5**) and 323-S_4-diBz (**L6**), while [16]aneS_4 was the 333-S_4-diBz (**L7**) macrocyclic analog.

Comparison of the structures of *trans*-[$RhCl_2$([16]aneS_4-diol)]$^+$ [11] and *trans*-[$RhCl_2$([16]aneS_4)]$^+$ [8] with *trans*-[$RhCl_2$-(333-S_4-diBz)]$^+$ demonstrated the added flexibility available to the acyclic ligands. These three structures contained only six-membered chelate rings to the Rh(III), with the acyclic ligand having one open end as well. For the two macrocycles, the Rh−S bond distances ranged from 2.348(3) to 2.354(2) Å with S−Rh−S bond angles ranging from 89.47(7) to 90.53(7)°, and the distances between S atoms ranging from 3.317(3) to 3.335(3) Å (Figure 7a).[8,11] The structure of *trans*-[$RhCl_2$(333-S_4-diBz)]$^+$ exhibited a wider range of Rh−S bond distances (2.329(2)−2.373(2) Å) and a much broader range of bond angles (82.82(6)−97.96(6)°). The S−S distances varied from 3.141(4) to

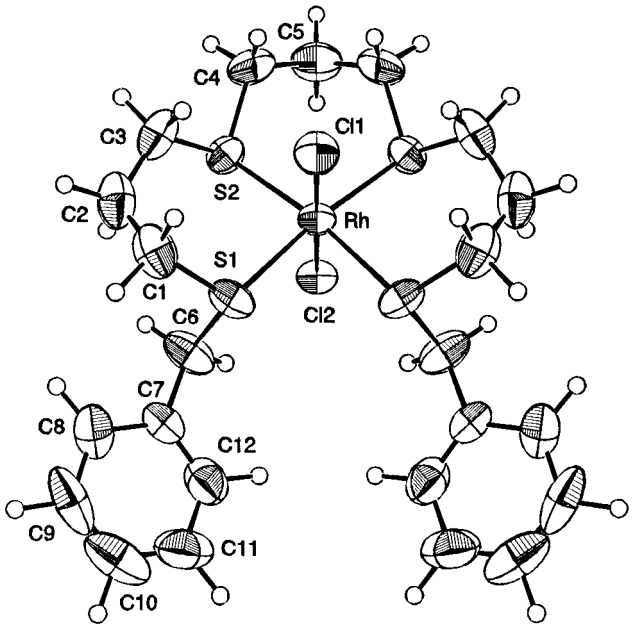

Figure 6. ORTEP representation (50% probability elipsoids) of *trans*-$[RhCl_2\mathbf{L7}]^+$.

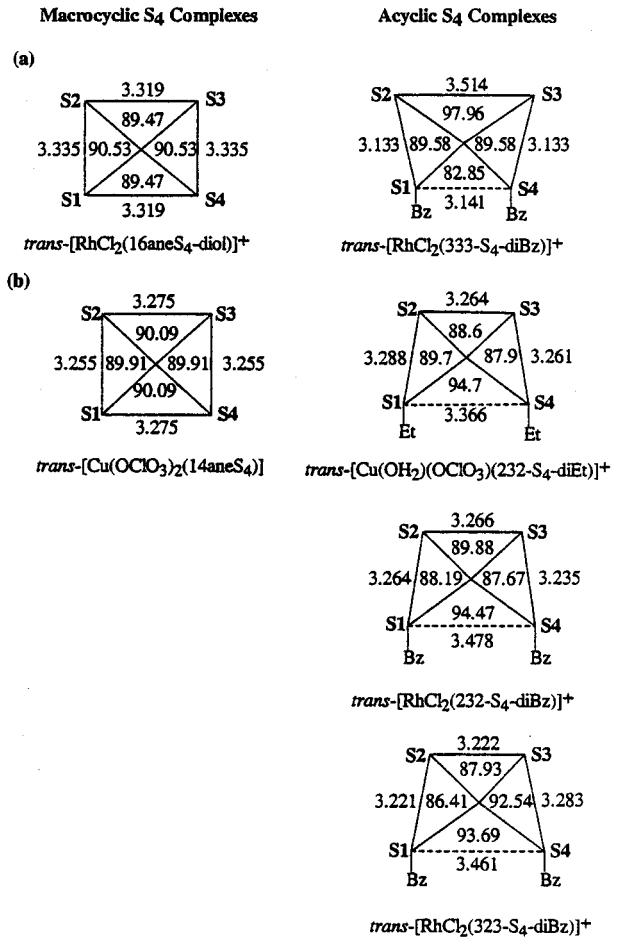

Figure 7. Comparison of the S−S distances and the S−M−S bond angles in analogous macrocyclic and acyclic tetrathioether complexes for (a) *trans*-$[RhCl_2(16aneS_4\text{-diol})]PF_6$[11] and *trans*-$[RhCl_2(333\text{-}S_4\text{-diBz})]PF_6$ and (b) *trans*-$[Cu(OClO_3)_2(14aneS_4)]$[37] and *trans*-$[Cu(OH_2)(OClO_3)(232\text{-}S_4\text{-diEt})]ClO_4$,[37] *trans*-$[RhCl_2(232\text{-}S_4\text{-diBz})]PF_6$, and *trans*-$[RhCl_2(323\text{-}S_4\text{-diBz})]PF_6$.

3.514(2) Å. The constraints (or rigidity) of the macrocycle required that all bond angles be comparable, while this was not necessary for the acyclic ligands. However, it was interesting to observe that the open end (S1−Rh−S4) of the 333-S_4-diBz complex exhibited the smallest angle while that directly opposite (S2−Rh−S3) had the largest angle. Minimization of steric interactions by the two benzyl moieties bonded to S1 and S4 probably contributed to this distortion, although one would expect a small expansion to occur simultaneously in all three of the remaining S−Rh−S angles.

Significant distortions were observed in the open end S−Rh−S angles for 232-S_4-diBz and 323-S_4-diBz, however, in both of these cases the S1−Rh−S4 angle has opened (to ca. 94°) rather than compressing as was observed for 333-S_4-diBz. Rh(III) has been reported to complex with [14]aneS_4 in only the *cis* configuration and thus direct comparison with Rh(III) situated in the cavity of this macrocycle is not possible.[8] However, comparison of the structures of *trans*-$[RhCl_2(232\text{-}S_4\text{-diBz})]^+$ and *trans*-$[RhCl_2(323\text{-}S_4\text{-diBz})]^+$ to the those reported for the Cu(II) complexes[37] with the related open chain (232-S_4-diEt) and macrocyclic ([14]aneS_4) tetrathioether ligands afforded insight to the cavity size expansion possible with the acyclic analogs (Figure 7b). The four S−Cu−S angles in $[CuX_2([14]aneS_4)]$ were close to 90° and all Cu−S bond distances were close to 2.30 Å.[37] Both the Rh and Cu structures with the acyclic analogs showed an expansion of the open end of the S_4 ligand framework, with the S−M−S angle being ca. 94° in both cases. However, M−S bond distances have not significantly changed. In the Rh structure, the two five-membered chelate rings undergo compression (decrease in the S−Rh−S angles) with the six-membered chelate ring (S2−Rh−S3) remaining close to 90° (Table 6). The benzyl groups bonded to S1 and S4 are oriented perpendicular to each other apparently to minimize steric interactions.

Stereochemistry at the Sulfur Centers in the Rh(III) Complexes. On coordination, each S atom becomes a chiral center and the stereochemistry about the S atoms play an important role in determining the conformation of the complexes. Each of the four S atoms on complexation with Rh(III) can exhibit either *R* or *S* stereochemistry. This leads to at least eleven different possible isomers for each *cis* or *trans* isomer, or five enantiomeric pairs of isomers and one meso isomer. The theoretical possibilities, listed as enantiomeric pairs, are *RRRR* and *SSSS*, *RSSS* and *SRRR*, *RRSS* and *SSRR*, *RSRR* and *SRSS*, *RSRS* and *SRSR*, and *RSSR* (meso). On the basis of the ORTEP drawings for the four X-ray crystal structures, the following stereochemistry was observed at the four S atoms.

ligand	geometry of Rh(III) complex	S1	S2	S3	S4
222-S_4-diBz	*cis*	*R*	*S*	*S*	*S*
232-S_4-diBz	*trans*	*R*	*R*	*S*	*R*
323-S_4-diBz	*trans*	*S*	*R*	*R*	*R*
333-S_4-diBz	*trans*	*S*	*R*	*S*	*R*

These four complexes crystallized in centrosymmetric space groups and thus the enantiomer for each complex was also present. It is interesting that the four complexes have different stereochemistries about the four S atoms and that only one of the theoretically possible stereoisomers was observed. With the exception of the 232-S_4 backbone in which both *cis* and *trans* isomers were observed for the complexes, the isomers listed were the only ones observed.

Dicarboxylic Acid−Tetrathioether−Rh(III) Complexes. As mentioned earlier, the chemistry of Rh(III) complexes with the dicarboxylic acid tetrathioether ligands is of particular interest because of their potential applications to therapeutic radiopharmaceuticals. The elemental analyses and the NMR spectra of the complexes with ligands **L1**−**L3** confirmed the

(37) Diaddario, L. L., Jr.; Dockal, E. R.; Glick, M. D.; Ochrymowycz, L. A.; Rorabacher, D. B. *Inorg. Chem.* **1985**, *24*, 356.

identities of these species. The assignments of the complexes as *cis* and/or *trans* was based on comparison with the spectroscopic data from the structurally characterized dibenzyl analogs. This included UV−visible, FT-IR, and NMR (^{1}H and ^{13}C) spectral analyses. The data obtained from the dicarboxylic acid complexes showed that they had the identical solution and solid state structures as their fully characterized dibenzyl−tetrathioether analogs. As for the dibenzyl analogs the d−d transitions observed in the electronic spectra were found to be characteristic of the geometry about the Rh(III) center, with longer wavelengths and lower ϵ values observed for the *trans* complexes (Table 2). The ^{13}C-NMR spectra of the complexes were indicative of the number of geometric isomers present in solution (Table 5), and the number of bands between 300 and 400 cm^{-1} in the FT-IR spectra supported the assignment of *cis* or *trans* (Tables 2 and 3). Combining these results allowed us to assign the geometries of the complexes as *cis*-[$RhCl_2$(222-S_4-diAcOH]-PF_6, *trans*-[$RhCl_2$(333-S_4-diAcOH]Cl, and a mixture of *cis* and *trans* isomers for [$RhCl_2$(232-S_4-diAcOH]Cl.

Conclusion

The Rh(III) complexes with dibenzyl and diacetic acid functionalized acyclic tetrathioether ligands (**L1**−**L7**) have been synthesized and characterized. The 1D and 2D NMR studies showed that the solution conformations of the Rh(III) complexes with ligands **L4**−**L7** were identical to those observed in the solid state. Single-crystal X-ray diffraction analysis of the Rh(III) complexes with the dibenzyl analogs (**L4**−**L7**) allowed us to assign the absolute configurations of these complexes, and allowed assignment of the structures of the analogous diacetic acid complexes based on comparative spectroscopic results as *cis*-[$RhCl_2$(222-S_4-diAcOH)]PF_6 (**L1**), *cis*/*trans*-[$RhCl_2$(232-S_4-diAcOH)]Cl (**L2**), and *trans*-[$RhCl_2$(333-S_4-diAcOH)]Cl (**L3**). Since radiopharmaceuticals must consist of a single, well-characterized species, complexes based on the acyclic 232-S_4 backbone are unsuitable because at least three different isomers were observed. Preliminary mouse biodistribution studies with the ^{105}Rh complexes of **L1** and **L3**, prepared using the methods previously described for ^{105}Rh−[16]aneS_4-diol,[11] show the primary clearance route to be through the kidneys (>85% of the injected dose in the bladder at 2 h for ^{105}Rh−**L1** and >73% for ^{105}Rh−**L3**). These results make them suitable for conjugation with a peptide or antibody fragment as there was no significant retention in any normal tissue.[38]

Acknowledgment. We gratefully acknowledge the support provided from the National Science Foundation NSF CHE 9011804 (X-ray facility) and 9221835 (250 MHz NMR).

Supporting Information Available: Tables giving experimental details, fractional coordinates, bond distances, bond angles, thermal parameters, torsion angles and least-squares planes for *cis*-[$RhCl_2$(222-S_4-diBz)]PF_6, *trans*-[$RhCl_2$(232-S_4-diBz)]PF_6, *trans*-[$RhCl_2$(323-S_4-diBz)]PF_6, and *trans*-[$RhCl_2$(333-S_4-diBz)]PF_6 (27 pages). Ordering information is given on any current masthead page.

IC960952Z

(38) Goswami, N.; Jurisson, S.; Alberto, R.; Volkert, W. A. Unpublished results.